VIP Archimedean Polyhedra Very Important Paper

International Edition: DOI: 10.1002/anie.201503609
German Edition: DOI: 10.1002/ange.201503609

Precise Molecular Fission and Fusion: Quantitative Self-Assembly and Chemistry of a Metallo-Cuboctahedron**

Ting-Zheng Xie, Kai Guo, Zaihong Guo, Wen-Yang Gao, Lukasz Wojtas, Guo-Hong Ning, Mingjun Huang, Xiaocun Lu, Jing-Yi Li, Sheng-Yun Liao, Yu-Sheng Chen, Charles N. Moorefield, Mary Jane Saunders, Stephen Z. D. Cheng, Chrys Wesdemiotis, and George R. Newkome**

Abstract: *Inspiration for molecular design and construction can be derived from mathematically based structures. In the quest for new materials, the adaptation of new building blocks can lead to unexpected results. Towards these ends, the quantitative single-step self-assembly of a shape-persistent, Archimedean-based building block, which generates the largest molecular sphere (a cuboctahedron) that has been unequivocally characterized by synchrotron X-ray analysis, is described. The unique properties of this new construct give rise to a dilution-based transformation into two identical spheres (octahedra) each possessing one half of the molecular weight of the parent structure; concentration of this octahedron reconstitutes the original cuboctahedron. These chemical phenomena are reminiscent of biological fission and fusion processes. The large 6 nm cage structure was further analyzed by 1D and 2D NMR spectroscopy, mass spectrometry, and collision cross-section analysis. New routes to molecular encapsulation can be envisioned.*

Nature exhibits highly symmetric polyhedral cage-like structures at different scales, such as viral capsids,[1] clatherin-coated vesicles,[2] and the protein transport complexes COP I and COP II.[3,4] All are connected mathematically by Archimedean polyhedra[5] and, from a synthetic-chemistry perspective, by the common thread of protein complex self-assembly. Inspired by both biomolecules and their underlying geometric principles, chemists have developed routes to create capsule and polyhedral assemblies that utilize hydrogen-bonding or coordination interactions.[6–10] Replicating large, multi-component, three-dimensional architectures in vitro is synthetically challenging, in part owing to the precise control necessary for building-block assembly and the fact that subtle changes in the subunits can lead to very different results.[8,11] Notable achievements towards the synthetic construction of very large cage-like constructs include cuboctahedra and dodecahedra[12] (5.2 and 7.5 nm, respectively, based on pulsed-gradient spin-echo NMR spectroscopy) and rhombicuboctahedra[8] and sphere-in-sphere rhombicuboctahedra[13] (5.0 and 6.3 nm, respectively, based on synchrotron X-ray crystallography).

The eloquent architecture of the protein complex COP II and its structural connection to Archimedean polyhedra provided inspiration for the design and construction of highly symmetric 3D supramolecular structures.[5,14,15] The molecular motif, critical parameters for the preciseness-of-fit of the building blocks, and the method of connectivity were considered. Ligand–metal–ligand building-block connectivity provides desirable synthetic characteristics by facilitating metal coordination sites to act as either vertices or edges in a contemplated shape.[13] The linearly coordinated, pseudo-octahedral {tpy–M^{2+}–tpy} complex (tpy = 2,2′:6′,2″-terpyridine) has been demonstrated to be a good option for the fabrication of 2D and 3D supramolecules.[16–18]

[*] Dr. T.-Z. Xie, Dr. K. Guo, Z. Guo, M. Huang, Dr. X. Lu, J.-Y. Li, Dr. C. N. Moorefield, Prof. S. Z. D. Cheng, Prof. C. Wesdemiotis, Prof. G. R. Newkome
Department of Polymer Science, The University of Akron
Akron, OH 44256 (USA)
E-mail: wesdemi@uakron.edu
newkome@uakron.edu
Dr. Y.-S. Chen
ChemMatCARS, The University of Chicago
Argonne, IL 60439 (USA)
W.-Y. Gao, Dr. L. Wojtas
Department of Chemistry, University of South Florida
4202 East Fowler Avenue, CHE205, Tampa, FL 33620 (USA)
Dr. G.-H. Ning
Department of Applied Chemistry, School of Engineering
The University of Tokyo (Japan)
Dr. M. J. Saunders
Department of Biological Sciences, Florida Atlantic University
Boca Raton, FL 33431 (USA)
Dr. S.-Y. Liao
Department of Applied Chemistry, Tianjin University of Technology
Tianjin 300384 (China)

[**] We gratefully acknowledge ChemMatCARS Sector 15, which is principally supported by the Divisions of Chemistry (CHE) and Materials Research (DMR) of the National Science Foundation (NSF/CHE-1346572), and the use of the Advanced Photon Source, an Office of Science User Facility operated by the U.S. Department of Energy (DOE) Office of Science at Argonne National Laboratory, which is supported by the U.S. DOE (DE-AC02-06CH11357). We also thank Lin Wang (Department of Chemistry, Zhejiang University) for help with the DOSY, HSQC, and HMBC NMR experiments, Dr. Matthew J. Panzner (Department of Chemistry, The University of Akron) for valuable discussions and insights into X-ray crystallography, and Chun Gao (Department of Chemistry, The University of Akron). G.R.N. and C.W. also acknowledge the National Science Foundation for support (CHE-1151991 and CHE-1308307, respectively).

Supporting information for this article is available on the WWW under http://dx.doi.org/10.1002/anie.201503609.

Using 2,2′:6′,2″-terpyridine as a readily available and easily functionalized monomer, we have reported the self-assembly of numerous 2D metallomacrocycles, including triangles,[19] hexagons,[20] a Sierpiński gasket,[21] and, most recently, a Sierpiński triangle,[22] wherein the vertices were connected through terpyridine-based coordination chemistry (Figure 1). Building on these mathematically derived shapes,

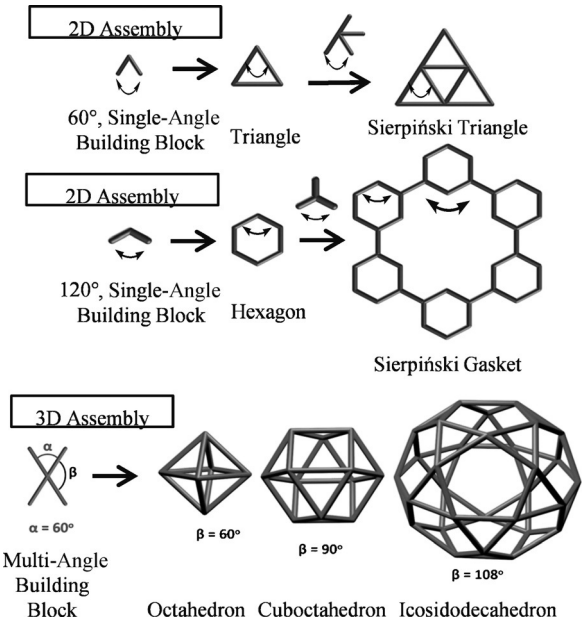

Figure 1. Construction of simple and complex 2D polygons, including a Sierpiński triangle and gasket, based on single-angle components and derivation of Archimedean polyhedra using multi-angle building blocks possessing increasingly greater angles (β). The critical dihedral angles within the cuboctahedron are 125°, which corresponds to $\beta = 90°$.

we herein describe the single-step, quantitative self-assembly of 3D, monodisperse metallospheres with a diameter of 6 mm, which are based on a classic Archimedean solid—the cuboctahedron—one of 13 convex polyhedra exhibiting two or more nonintersecting regular convex polygons arranged such that all sides are of equal length.[5] The requisite building block for this semi-regular polygon was designed by considering an X-shaped molecular building block that could be mapped onto the vertices of a cuboctahedron and impart the desired angles, α and β, with values of 60° and 90°, respectively (Figure 1). Notably, the appropriate molecular construct will introduce a cumulative shape-persistent memory effect that translates to the subsequent architectural assembly.

The use of an Archimedean-inspired monomer ($\beta = 90°$) to facilitate the self-assembly of a cuboctahedron cage requires the generation of 24 edges and 12 vertices, which form the basis of 14 total faces comprising 8 triangles and 6 squares, all predicated on 24 dihedral angles equal to 125°. An exhaustive literature search in combination with molecular modeling studies suggested that an ethano-bridged anthracene with directed substituted terpyridine connectors would provide a phenyl-mediated, 60° angled, *ortho* substitution pattern leading to the triangular faces. The bridged ethanoanthracene possesses an ideal 127° angle, which ultimately results in the requisite 90° β angle necessary to form the desired square faces and is very close to the targeted 125° dihedral component.

The tetrakis(terpyridinyl) ligand **3** was prepared (67%) using a Suzuki coupling reaction by treatment of 2,3,6,7-tetrakis(4-bromophenyl)-9,10-dimethyl-9,10-ethanoanthracene (**1**), which was obtained by the direct bromination (Br_2) of commercially available 9,10-dimethyl-9,10-ethanoanthracene, with four equivalents of 4-(2,2′:6′,2″-terpyridinyl)phenylboronic acid (**2**).[23] The ^{1}H NMR spectrum of ligand **3** exhibited one set of expected signals that were attributed to the terpyridinyl moieties and a single set of peaks assigned to the newly introduced aryl groups, suggesting free rotation throughout the two sets of 60° juxtaposed arms (Figure 2).

The one-step self-assembly (Figure 2) of monomer **3** with a precise ratio (1:2) of $Zn(NO_3)_2$ in a stirred mixture of MeOH and $CHCl_3$ (1:1, v/v) at 25° for one hour led to a translucent pale-yellow solution, which gave (>98%) the desired compound **4** as a light-yellow precipitate when treated with saturated aqueous NH_4PF_6 (to exchange NO_3^- for PF_6^-); the structure of **4** was subsequently confirmed by 1D, 2D, and DOSY NMR spectroscopy, ESI-TWIM mass spectrometry [electrospray ionization mass spectrometry coupled with traveling-wave ion mobility spectrometry (TWIM-MS), a variant of ion mobility spectrometry], TEM imaging, and single-crystal X-ray crystallography. Notably, characterization of the more labile Cd^{2+} analogue **5** mirrored that of the Zn^{2+}-based sphere **4**, with the exception of overlapping of the 4,4″- and 6,6″-tpy hydrogen atoms and the outermost aryl hydrogen atoms in the ^{1}H (H_a for **3**, Figure 2) and COSY NMR spectra; the MS data are essentially identical (Supporting Information, Figures S7 and S12).

The ^{1}H NMR spectrum of **4** [in $[D_7]$DMF and CD_3CN (1:4, v/v); Figure 2] exhibited a single set of sharp peaks, which indicates the formation of a single and highly symmetric species in which all identically positioned nuclei are chemically and magnetically equivalent. The COSY and NOESY NMR experiments were used to aid and verify the assignments of the ^{1}H NMR spectrum.

The expected upfield shift of the doublet from 8.75 to 7.95 ppm ($\Delta\delta = 0.8$ ppm), attributed to the 6,6″-tpy hydrogen atoms, is indicative of the formation of the pseudo-octahedral bis(terpyridine) complex and the resultant positioning of the H6 atoms near the aromatic ring current of the perpendicularly opposed terpyridine. All other signals show the characteristic downfield shifts following complex formation. Notably, the large, rigid complex **4** displays a ^{1}H NMR spectrum that is well-resolved with sharp, easily assignable peaks with only the methyl and bridging methylene protons exhibiting broadening, in contrast to other cage-like pyridine palladium complexes.[8]

The ^{1}H 2D DOSY NMR spectrum of complex **4** (Figure S11) clearly shows a single band with a diffusion coefficient $D = 1.99 \times 10^{-10}$ ($\log D = -9.69$), along with a corresponding solvent band ($\log D = -8.40$), indicative of a single species in the $[D_7]$DMF/CD_3CN (1:4, v/v) solution. The calculated diameter of the spherical complex, according to the

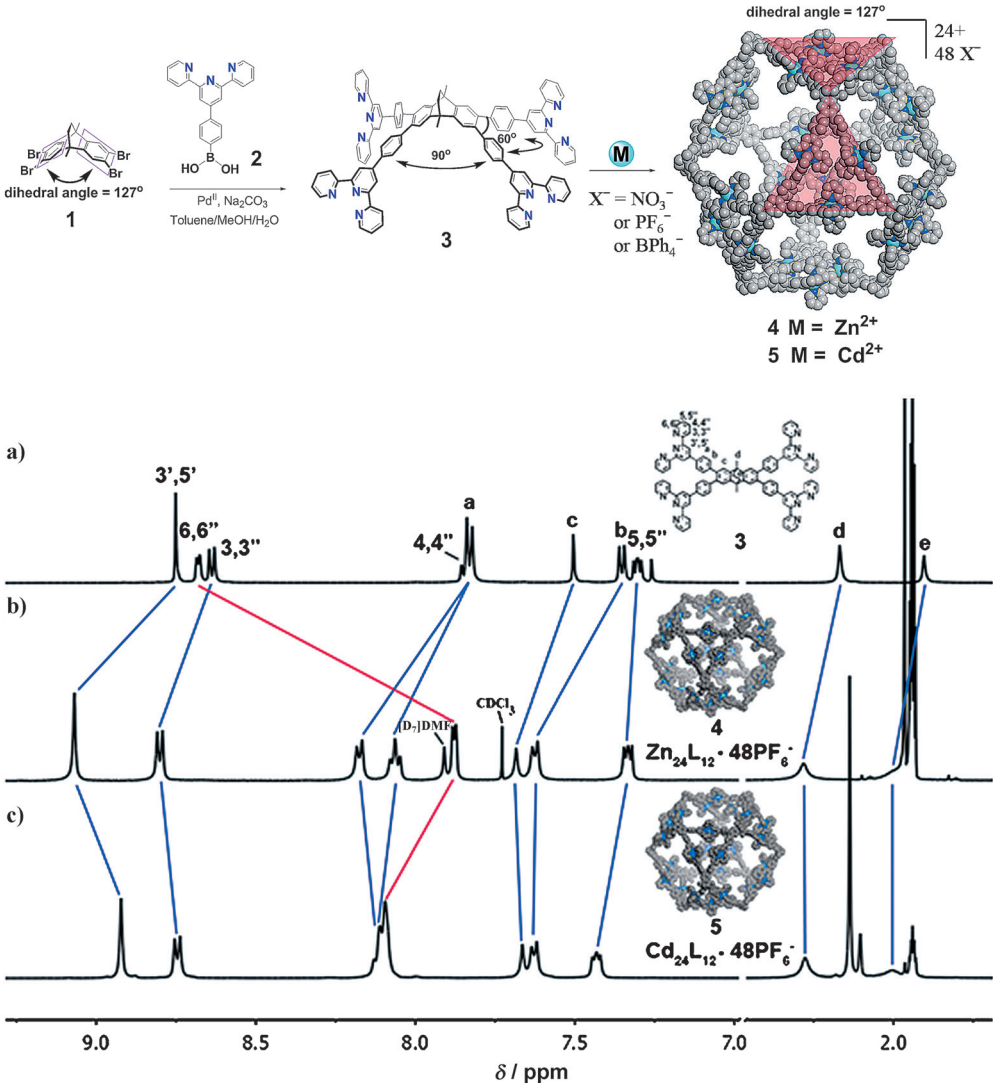

Figure 2. Top: Synthesis of the ethano-bridged tetrakis(terpyridine) monomer **3** and the Zn^{2+}- and Cd^{2+}-based cuboctahedra **4** and **5**. The critical dihedral angle (127°) depicted for **1** is translated and instilled into tetrakis(terpyridine) **3** and the resulting cages **4** and **5**. Bottom: ^{1}H NMR spectra (500 MHz, 300 K) of monomer **3** (a) in $CDCl_3$ and complexes **4** (b) and **5** (c) in $CD_3CN/[D_7]DMF$ (4:1, v/v).

viscosity of these mixed solvents measured before (0.00422 poise),[24] is 5.18 nm, which is fully consistent and in agreement with the modeling of the structure as well as with the TEM results.

The ESI mass spectrum of the $[24\{tpy{-}Zn^{2+}{-}tpy\}]\cdot[48\,PF_6^-]$ complex **4** (Figure S12) further supports the structure of the cuboctahedron by revealing a series of dominant peaks at *m/z* 942.3, 989.6, 1041.2, 1097.7, 1159.9, and 1228.6, corresponding to charge states ranging from 24+ to 19+, respectively. These MS results provide strong support for the combination of 12 ligands and 24 Zn^{2+} metal ions along with the experimental *m/z* values for each charge state and are consistent with the corresponding calculated values. Additional support (Figure S12) for **4** was provided by ESI-TWIM MS experiments.[25] TWIM-MS resembles molecular separation, such as chromatography, separating ions by their charge and shape/size in the TWIM region, followed by *m/z* in the adjoining mass analyzer. This method serves as a unique complement to more traditional characterization procedures as it enables the resolution of isomeric ions and the determination of structural information.[26–28] The TWIM mass spectrum exhibits charge states ranging from 24+ to 19+ derived from **4**, with a single and narrow band for each charge state and a narrow drift time distribution for the signals extracted for each band, clearly indicating the presence of a single species; this finding is consistent with the NMR results.

The stability of complex **4** was probed with gradient tandem MS (gMS^2). The 19+, 11+, and 8+ ions (corresponding to *m/z* values of 1228, 2227, and 3116, respectively) were isolated and subjected to collisionally activated dissociation (CAD) with Ar gas prior to ion mobility separation at collision energies ranging from 10 to 100 eV. The cuboctahedron exhibits good stability, in agreement with other highly charged ions of $\{tpy{-}Zn^{2+}{-}tpy\}$ complexes.[29] Only when the collision energy reached 37 eV, the 19+ complex ion (*m/z* 1228) completely disappeared, yielding several fragments. Notably, ions with lower charges exhibited excellent stability in gMS^2 experiments; for example, the 8+ ion (*m/z* 3116) did not completely disappear until the collision energy reached 95 eV. This finding suggests that the stability of the complex is greater with a higher number of "protective" surrounding anions.

Suitable, colorless, cubic single crystals for X-ray analysis (Figure 3) were obtained after two months by vapor diffusion of EtOAc into a DMF/MeCN (1:1, v/v) solution of complex **4**. Crystals in the mother liquor were sealed in a quartz capillary and maintained at 25 °C during data collection using synchrotron X-ray radiation. Owing to the large volume of the spherical complex (in the size range of small proteins) and the high number of disordered counterions and solvent molecules, the diffraction spots, not unexpectedly, were observed only to a resolution of approximately 1.6 Å. It was, however, sufficient to model the positions of the essential core elements of the 12 ligands and the 24 Zn^{2+} ions, thereby leading to the

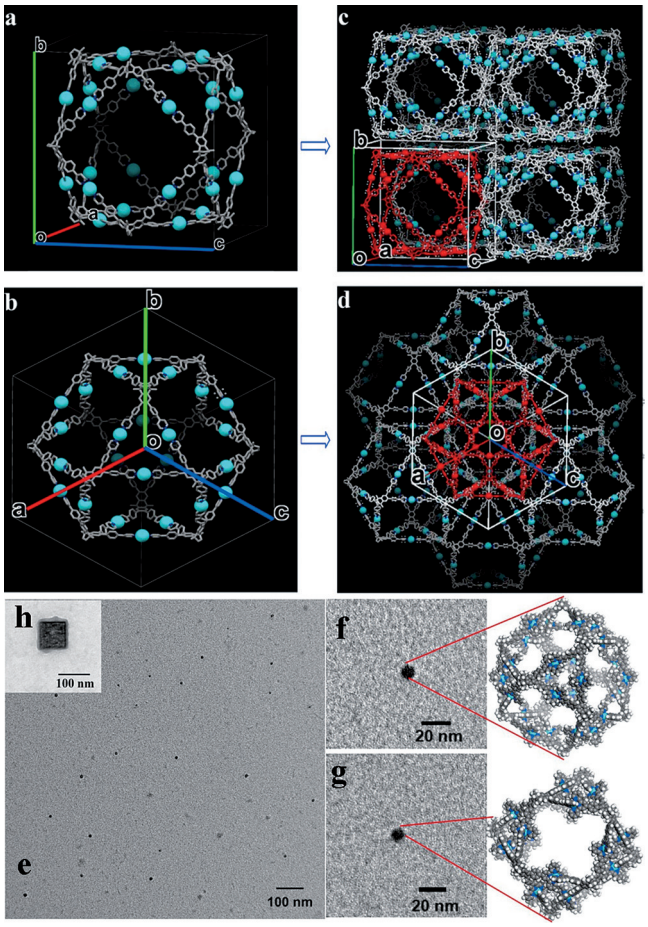

Figure 3. Top: Single-crystal structure[39] of complex **4** viewed a) from an angle relative to the *ac* plane [the (−6.23 1 1.96) direction] and b) along the diagonal [the (111) direction]. c, d) The packing of eight molecules viewed as described in (a) and (b), respectively. The cuboctahedron molecules pack into a cubic crystal in the cubic space group. The outer adjacent pyridinyl rings of each of the 48 terpyridine triads were highly disordered; thus, these groups along with all of the hydrogen atoms have not been included in the structural model that is based on X-ray diffraction. Crystal data: Space group $Pm\bar{3}m$, $a=b=c=47.881(1)$ Å, $V=109\,772(34)$ Å^3, $Z=1$. Residual $R1=0.1827$ [$I>2\sigma(I)$] and goodness of fit = 1.039 for $Zn_{24}L_{12}^{48+}\cdot 48\,PF_6^-$ ($C_{1224}H_{840}F_{288}N_{144}P_{48}Zn_{24}$, 26 092.85 D). Bottom: TEM images of complex **4** showing a homogeneous field of similarly sized objects (e) whereas higher-magnification images display the classic cuboctahedron hexagonal (f) and cubic shapes (g). Furthermore, images were obtained that show the higher-order packing potential of **4**; the cube in the inset (h) is estimated to contain 19 molecules on one side.

cuboctahedral structure of complex **4**, which is consistent with the computer-generated model. As expected, a highly symmetric and shape-persistent structure showing the 14 faces with the requisite 24 edges and 12 vertices was revealed, supporting the classic cuboctahedron structure with O_h symmetry. The 24 metal atoms form a rhombicuboctahedron conformation with triangles and unequal-sided rectangles in which the greatest distance between two Zn^{2+} ions is 4.9 nm, the average distance across the interior is approximately 40 Å, and the inner void volume is about 46 800 Å^3.

Further evidence confirming the cuboctahedron's structure was provided by collision cross-section (CCS) data as determined from the drift times measured in the TWIM-MS experiments (Table S1). CCS can be viewed as the rotationally averaged forward-moving surface area of the cuboctahedron. For the 15+, 17+, and 20+ charge states of cage **4**, the CCSs are 3014.2, 2983.8, and 2888.5 Å^2, respectively. The slight CCS differences between these three charge states (balanced by 33, 31, and 28 PF_6^- counterions, respectively) indicate that **4** possesses a rigid and shape-persistent architecture. The average experimental CCS (2931.3 Å^2) agrees well with the theoretically predicted CCS for the counterion-free complex (2720 Å^2), which was calculated from the corresponding energy-minimized structure using the trajectory method,[30–34] which rigorously considers the collision process between ions and buffer gas in the ion-mobility region. The differences between the experimental and theoretical CCS values are most likely due to the effect of the anions. From the data in Table S1, the experimental CCS gradually decreases with increasing charge, suggesting that the anions contribute less to the CCS at high charge densities.

Transmission electron microscopy (TEM) facilitated the visualization of metallomacrocyclic cage **4**, directly revealing both the size and shape of individual molecules upon deposition of a dilute MeCN/DMF (10^{-7} M, 4:1, v/v) solution of **4** with PF_6^- counterions on carbon-coated grids (Cu, 400 mesh; Figure 3e). At higher magnification, the images of single molecules, poised on different faces, exhibit the hexagonal and cubic shapes defined by cuboctahedron architecture (Figure 3f,g). The ability of these polymetallic complexes to pack into aggregates was confirmed with the observation of large, regular, cubic species (Figure 3h), where in the pictured case, 19 molecules are estimated to be arranged linearly on each edge.

Recently, during our self-assembly studies, it was observed that a smaller supramolecular bis(rhombus) possessing a disc-shaped, spoked-wheel motif and {tpy–Cd^{2+}–tpy} connectivity, underwent molecular fission to generate exactly two equivalents of a new tetrahedron, each characterized by precisely one half of the original molecular weight,[29] following its dilution. Interestingly, upon concentration, this tetrahedron underwent molecular fusion to reconstitute the original bis(rhombus) construct. Thus, subsequent dilution of this larger Zn^{2+}-based cuboctahedron **4** resulted in a poorly resolved ESI mass spectrum (not shown), which still indicated the presence of a new species possessing half the molecular weight of **4**. Accordingly, diluting the Cd^{2+} cuboctahedron **5**, possessing the more labile {tpy–Cd^{2+}–tpy} connectivity, using PF_6^- counterions, led to a mixture of **5** and the low-molecular-weight species **6**; further dilution converted the bulk of the material into a octahedral structure **6**, consisting of 12 Cd^{2+} and 24 PF_6^- ions. ESI-MS was subsequently employed to follow the postulated transformation of sphere **5** from one motif into the smaller sphere **6a** (Figure 4a–c and Figures S13 and S15). Attempts to isolate and fully characterize this new structure subsequently focused on the use of different counterions during the self-assembly reactions.

Upon switching the counterion from PF_6^- to BPh_4^-, the same ligand self-assembled to give (> 95%) exclusively the octahedral cage-shaped complex **6b**, which was readily confirmed by NMR spectroscopy (Figure 4f,g) and ESI-

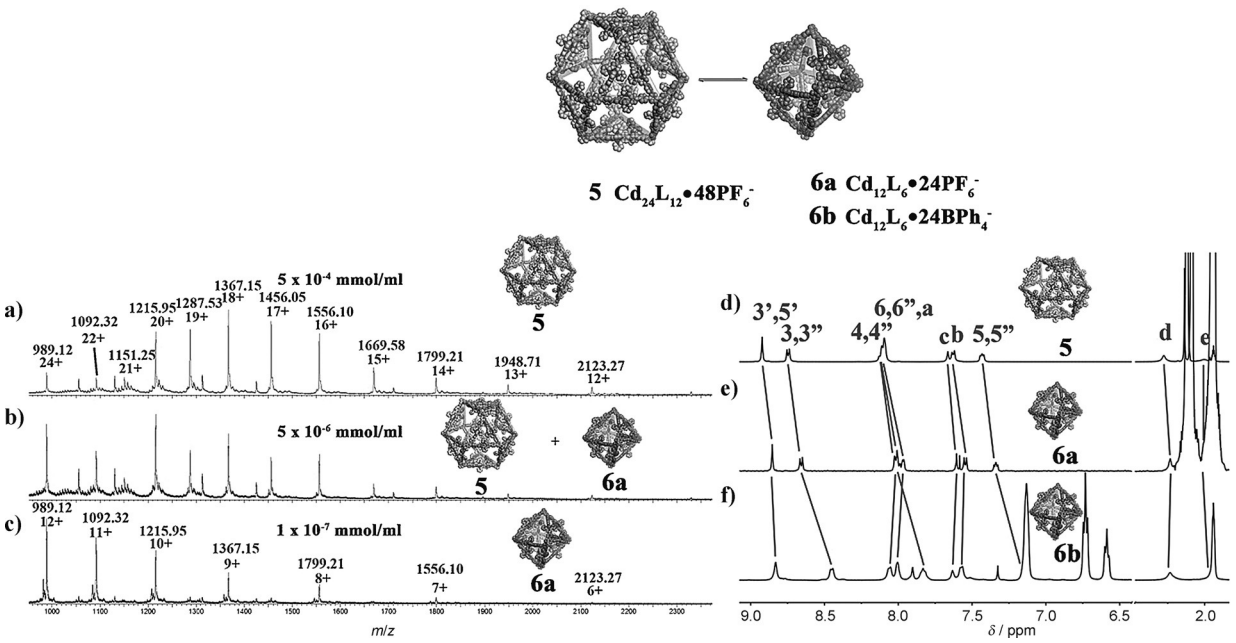

Figure 4. Left: ESI-MS spectra of the cuboctahedron (a, 5×10^{-4} mmol mL^{-1}), the cuboctahedron–octahedron mixture obtained upon dilution of the cuboctahedron (b, 5×10^{-6} mmol mL^{-1}), and the octahedron architecture ultimately obtained upon further dilution (c, 1×10^{-7} mmol mL^{-1}). Right: The dynamic equilibrium between cuboctahedron **5** ($Cd_{24}L_{12}$) and octahedron **6** ($Cd_{12}L_6$). Pertinent ^{1}H NMR spectra of d) cuboctahedron-shaped complex **5** with PF_6^- as the anion (CD_3CN, 5×10^{-4} mmol L^{-1}), e) octahedron-shaped complex **6a** with PF_6^- as the anion (CD_3CN, 1×10^{-4} mmol L^{-1}), and f) octahedron-shaped complex **6b** with BPh_4^- as the anion (CD_3CN/[D_7]DMF, 4:1, v/v, 5×10^{-4} mmol L^{-1}).

TWIM-MS (Figures S14 and S16). The ^{1}H NMR spectrum of complex **6b** exhibited a well-resolved set of signals with the symmetry (Figure 4 f) that is expected for the octahedron and indicative of a single species possessing a high degree of molecular symmetry. Notably, all of the ^{1}H NMR peaks showed upfield shifts relative to the spectrum of the cuboctahedron.

Therefore, the cuboctahedron is favored at higher concentrations, and upon dilution, molecular fission gives rise to two equivalents of the octahedron **6**, whereas upon concentration, molecular fusion regenerates the original cuboctahedron **5**.[35] The number of particles in the unit volume decreased correspondingly until entropic forces[36–38] pushed the self-assembled complex to switch into the smaller octahedron structure. We conclude that entropy plays a critical role in this example of molecular fusion and fission as the very large structural interchanges can be induced by changing either the size of the counterions or compound concentration.

In summary, we have employed a retrosynthetic analysis of an Archimedean polyhedron to design and synthesize a terpyridine-based, cuboctahedron-shaped supramacromolecule in the single-step self-assembly of 12 novel tetradentate terpyridinyl ligands with 24 Zn^{2+} ions. Unequivocal traditional characterization was accomplished, and its single-crystal X-ray structure was determined. This nanoscale [24{tpy–Zn^{2+}–tpy}][48PF_6^-] cuboctahedron (**4**) with its large cavity shows great potential for drug transport and host–guest chemistry, as suggested by its similarity to known biological protein complexes, such as clatherin, COP I, and COP II, which are involved in cellular vesicle creation. The novel dynamic structural interconversion of its corresponding Cd^{2+} complex with the same ligand occurs between two different structures, which are cuboctahedron-shaped [24{tpy–Cd^{2+}–tpy}][48PF_6^-] (**5**) and octahedron-shaped [12{tpy–Cd^{2+}–tpy}][24PF_6^-] (**6**). These molecular-level fission and fusion processes could be easily tuned by simply changing the concentration; the use of differently sized counterions can also play an important role for the overall structural stability. Furthermore, this synthetic method gives access to large multicomponent architectures that mimic biological molecules using easily synthesized Archimedean-prescribed monomers, thus adding a new series of nanoscale building blocks to the material sciences.

Keywords: Archimedean polyhedra · self-assembly · shape-persistent macromolecules · supramolecular chemistry

How to cite: *Angew. Chem. Int. Ed.* **2015**, *54*, 9224–9229
Angew. Chem. **2015**, *127*, 9356–9361

[1] G. Vernizzi, M. O. Cruz, *Proc. Natl. Acad. Sci. USA* **2007**, *104*, 18382–18386.
[2] H. T. McMahon, E. Boucrot, *Nat. Rev. Mol. Cell Biol.* **2011**, *12*, 517–533.
[3] S. M. Stagg, C. Gürkan, D. M. Fowler, P. LaPointe, T. R. Foss, C. S. Potter, B. Carragher, W. E. Balch, *Nature* **2006**, *439*, 234–238.
[4] The Nobel Prize in Physiology or Medicine 2013, http://www.nobelprize.org/nobel_prizes/medicine/laureates/2013/ (accessed: March 3rd, 2015).
[5] E. W. Weisstein, Archimedean solid, MathWorld - A Wolfram Web Resource, http://mathworld.wolfram.com/ArchimedeanSolid.html.

[6] B. Olenyuk, J. A. Whiteford, A. Fechtenkötter, P. J. Stang, *Nature* **1999**, *398*, 796 – 799.
[7] L. R. MacGillivray, J. L. Atwood, *Nature* **1997**, *389*, 469 – 472.
[8] Q.-F. Sun, J. Iwasa, D. Ogawa, Y. Ishido, S. Sato, T. Ozeki, Y. Sei, K. Yamaguchi, M. Fujita, *Science* **2010**, *328*, 1144 – 1147.
[9] Y. Liu, C. Hu, A. Comotti, M. D. Ward, *Science* **2011**, *333*, 436 – 440.
[10] S. Pasquale, S. Sattin, E. C. Escudero-Adán, M. Martínez-Belmonte, J. de Mendoza, *Nat. Commun.* **2012**, *3*, 785.
[11] C. Gütz, R. Hovorka, C. Klein, Q.-Q. Jiang, C. Bannwarth, M. Engeser, C. Schmuck, W. Assenmacher, W. Mader, F. Topić, K. Rissanen, *Angew. Chem. Int. Ed.* **2014**, *53*, 1693 – 1698; *Angew. Chem.* **2014**, *126*, 1719 – 1724.
[12] B. Olenyuk, M. D. Levin, J. A. Whiteford, J. E. Shield, P. J. Stang, *J. Am. Chem. Soc.* **1999**, *121*, 10434 – 10435.
[13] Q.-F. Sun, T. Murase, S. Sato, M. Fujita, *Angew. Chem. Int. Ed.* **2011**, *50*, 10318 – 10321; *Angew. Chem.* **2011**, *123*, 10502 – 10505.
[14] K. Harris, D. Fujita, M. Fujita, *Chem. Commun.* **2013**, *49*, 6703 – 6712.
[15] T. R. Cook, Y.-R. Zheng, P. J. Stang, *Chem. Rev.* **2013**, *113*, 734 – 777.
[16] T. Schröder, R. Brodbeck, M. M. C. Letzel, A. Mix, B. Schnatwinkel, M. Tonigold, D. Volkmer, J. Mattay, *Tetrahedron Lett.* **2008**, *49*, 5939 – 5942.
[17] C. Wang, X.-Q. Hao, M. Wang, C. Guo, B. Xu, E. N. Tan, Y. Y. Zhang, Y. Yu, Z.-Y. Li, H.-B. Yang, M.-P. Song, X. Li, *Chem. Sci.* **2014**, *5*, 1221 – 1226.
[18] T.-Z. Xie, S.-Y. Liao, K. Guo, X. Lu, X. Dong, M. Huang, C. N. Moorefield, S. Z. D. Cheng, X. Liu, C. Wesdemiotis, G. R. Newkome, *J. Am. Chem. Soc.* **2014**, *136*, 8165 – 8168.
[19] A. Schultz, Y. Cao, M. Huang, S. Z. D. Cheng, X. Li, C. N. Moorefield, C. Wesdemiotis, G. R. Newkome, *Dalton Trans.* **2012**, *41*, 11573 – 11575.
[20] G. R. Newkome, T. J. Cho, C. N. Moorefield, G. R. Baker, R. Cush, P. S. Russo, *Angew. Chem. Int. Ed.* **1999**, *38*, 3717 – 3721; *Angew. Chem.* **1999**, *111*, 3899 – 3903.
[21] G. R. Newkome, P. Wang, C. N. Moorefield, T. J. Cho, P. P. Mohapatra, S. Li, S.-H. Hwang, O. Lukoyanova, L. Echegoyen, J. A. Palagallo, V. Iancu, S.-W. Hla, *Science* **2006**, *312*, 1782 – 1785.
[22] R. Sarkar, K. Guo, C. N. Moorefield, M. J. Saunders, C. Wesdemiotis, G. R. Newkome, *Angew. Chem. Int. Ed.* **2014**, *53*, 12182 – 12185; *Angew. Chem.* **2014**, *126*, 12378 – 12381.
[23] J.-L. Wang, X. Li, X. Lu, I.-F. Hsieh, Y. Cao, C. N. Moorefield, C. Wesdemiotis, S. Z. D. Cheng, G. R. Newkome, *J. Am. Chem. Soc.* **2011**, *133*, 11450 – 11453.
[24] D. S. Gill, H. Anand, A. Kumari, J. K. Puri, *Z. Naturforsch. A* **2004**, *59*, 615 – 620.
[25] X. Li, Y.-T. Chan, G. R. Newkome, C. N. Wesdemiotis, *Anal. Chem.* **2011**, *83*, 1284 – 1290.
[26] S. Perera, X. Li, M. Soler, A. Schultz, C. Wesdemiotis, C. N. Moorefield, G. R. Newkome, *Angew. Chem. Int. Ed.* **2010**, *49*, 6539 – 6544; *Angew. Chem.* **2010**, *122*, 6689 – 6694.
[27] C. S. Hoaglund-Hyzer, A. E. Counterman, D. E. Clemmer, *Chem. Rev.* **1999**, *99*, 3037 – 3079.
[28] E. R. Brocker, S. E. Anderson, B. H. Northrop, P. J. Stang, M. T. Bowers, *J. Am. Chem. Soc.* **2010**, *132*, 13486 – 13494.
[29] X. Lu, X. Li, K. Guo, T.-Z. Xie, C. N. Moorefield, C. Wesdemiotis, G. R. Newkome, *J. Am. Chem. Soc.* **2014**, *136*, 18149 – 18155.
[30] A. A. Shvartsburg, M. F. Jarrold, *Chem. Phys. Lett.* **1996**, *261*, 86 – 91.
[31] M. F. Jarrold, *Annu. Rev. Phys. Chem.* **2000**, *51*, 179 – 207.
[32] A. A. Shvartsburg, B. Liu, K. W. M. Siu, K.-M. Ho, *J. Phys. Chem. A* **2000**, *104*, 6152 – 6163.
[33] F. Lanucara, S. W. Holman, C. J. Gray, C. E. Eyers, *Nat. Chem.* **2014**, *6*, 281 – 294.
[34] Y.-T. Chan, X. Li, J. Yu, G. A. Carri, C. N. Moorefield, G. R. Newkome, C. Wesdemiotis, *J. Am. Chem. Soc.* **2011**, *133*, 11967 – 11976.
[35] M. L. Saha, S. Pramanik, M. Schmittel, *Chem. Commun.* **2012**, *48*, 9459 – 9461.
[36] M. Fujita, O. Sasaki, T. Mitsuhashi, T. Fujita, J. Yazaki, K. Yamaguchi, K. Ogura, *Chem. Commun.* **1996**, 1535 – 1536.
[37] T. Kraus, M. Budšěínský, J. Cvačka, J.-P. Sauvage, *Angew. Chem. Int. Ed.* **2006**, *45*, 258 – 261; *Angew. Chem.* **2006**, *118*, 264 – 267.
[38] M. Schweiger, S. R. Seidel, A. M. Arif, P. J. Stang, *Inorg. Chem.* **2002**, *41*, 2556 – 2559.
[39] CCDC 1050911 contains the supplementary crystallographic data for this paper. These data are provided free of charge by The Cambridge Crystallographic Data Centre.

Received: April 20, 2015
Published online: June 11, 2015

